Journal of Materials Chemistry C

Accepted Manuscript

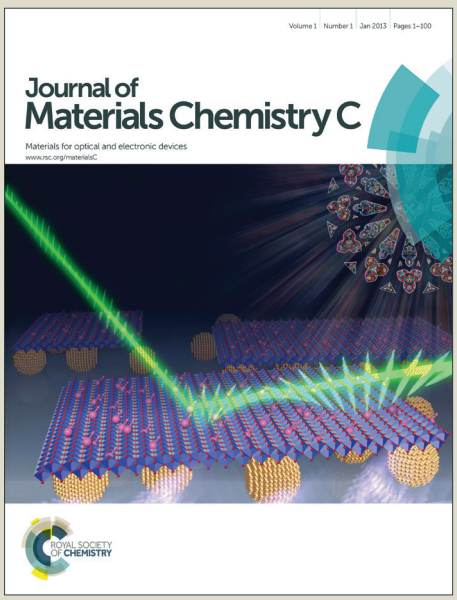

ROYAL SOCIETY OF CHEMISTRY

www.rsc.org/materialsC

Journal of Materials Chemistry C

ARTICLE

1,3,5-triazine based polymer as nonlinear near-infrared antenna for two-photon activated volumetric optical memories

Received 00th January 20xx,
Accepted 00th January 20xx

DOI: 10.1039/x0xx00000x

www.rsc.org/

I. F. A. Mariz,*[a] F. Siopa[b], C. A. B. Rodrigues[b], C.A.M. Afonso[b], X.Chen[c], J.M.G. Martinho[a] and E. M.S.Maçôas*[a]

The ability of a 1,3,5-triazine based polymer to work as a nonlinear near-infrared (NIR) antenna in functional optical materials is discussed. The push-pull polymer is composed of alternating electron acceptor cores of 2,4,6-tris(thiophen-2-yl)-1,3,5-triazine, bridged by electon donor groups of 9,9-dihexyl-9H-fluorene. It has been tailored for high two-photon absorption and efficient up-convertion of the excitation energy into fluorescence emission. These properties are here explored in the operation of prototypical storage material for volumetric nonlinear optical memories. Multilayer data storage is demonstrated in composite films of photochromic (PC) molecules doped with the polymer. The two-photon excitation of the polymer triggers a unidirectional isomerization of the PC molecules (a cycloreversion process from the closed to the open isomer) via Förster resonant energy transfer. Data recording with as little as 1 ms of exposure time and 1mW of 740 nm radiation is accomplished.

Introduction

The intrinsic spatial localization of multiphoton induced processes, provided by their nonlinear dependence on the light intensity, has been successfully explored in many applications, such as multiphoton fluorescence microscopy,[1-4] optical power limiting,[5] and high-density optical data storage[6]. Due to the reduced scattering of longer wavelengths (Rayleigh scattering cross-section scales with λ^{-4}), the near-infrared (NIR) light used in multiphoton excitation is able to penetrate deeper into thick and scattering samples, when compared to excitation in the ultraviolet and visible regions of the electromagnetic spectrum. These two properties (spatial confinement and penetration depth) are at the heart of the multilayer writing and addressing strategy for increasing the density of optical data storage media,[7-14] competing directly with efforts made towards decreasing the bit size by reducing the excitation wavelength and/or using sophisticated super-resolution methods.[15]

In the design of nonlinear functional materials, optimized two-photon absorbers are used as nonlinear NIR-antenna, and combined with active units (e.g. sensors and biologically active units) to perform specific tasks upon demand.[16] In multilayer data storage applications, such design strategy has led to the combination of NIR-antenna with photochromic units.[14, 17] Recently, the nonlinear emission properties of 1,3,5-triazine derivatives have been systematically studied. The triazine unit is remarkable in the context of supramolecular interactions (able to interact via coordination bonds, hydrogen bonding, electrostatic and charge-transfer effects, and aromatic–stacking), with applications in host-guest chemistry, catalysis, anion recognition, sensors, electronics and magnetism. [18-20] Its strong electron accepting ability and good coplanarity with peripheral aromatic groups is of particular relevance to the present study. Such properties have been explored in the optimization of triazine derivatives towards high two-photon brightness, combining high two-photon absorption (TPA) cross-sections with high emission quantum yields. A myriad of architectures have been considered, from octupolar molecules to linear and hyperbranched polymers, and polymer nanoparticles.[21-27] These studies suggested that a linear polymer framework with alternating push-pull units having the 2,4,6-tris(thiophen-2-yl)-1,3,5-triazine fragment as the electron-acceptor would be better for the design of efficient nonlinear NIR-antenna. Such arrangement has led to TPA cross-sections in the 10^3-10^4 GM range, with mass-weighted TPA cross-sections of 1.1 GM.mol/g (almost double that of analogous octupolar molecules, 0.63 GM.mol/g) and high emission quantum yields (up to 0.7).[22]

To widen the field of application of triazine polymers to data storage, a linear polymer with alternating electron acceptor (2,4,6-tris(thiophen-2-yl)-1,3,5-triazine) and donor (9,9-dihexyl-9H-fluorene) units, with high TPA cross-section (TPA-

[a] Centro de Química-Física Molecular and IN-Institute of Nanoscience and Nanothecnology, Instituto Superior Técnico, Av. Rovisco Pais, 1049-001 Lisboa, Portugal.Email: ines.mariz@tecnico.ulisboa.pt and Email: Ermelinda.macoas@tecnico.ulisboa.pt
[b] Research Institute for Medicines (iMed.ULisboa), Faculty of Pharmacy, University of Lisbon. Av. Prof. Gama Pinto, 1649-003 Lisbon, Portugal
[c] Hubei Key Laboratory on Organic and Polymeric Opto-electronic Materials, College of Chemistry and Molecular Sciences, Wuhan University, Wuhan 430072, China. Fax: 86-27-68756757.
Electronic Supplementary Information (ESI) available.. See
DOI: 10.1039/x0xx00000x

polymer), is here combined with 1,2-bis(2-methyl-benzo[b]thiophen-3-yl)hexa-fluorocyclopentene, a well-known photochromic (PC) molecule with two photochemically interconvertible isomers (**Fig. 1**).[28] The PC belongs to the diarylethene family, one of the most efficient photochromic systems in the solid state, with excellent fatigue resistance, high photoisomerization quantum yields for both the cyclization and cycloreversion processes, and thermal stability.[28, 29] Its application in volumetric data storage is hindered by either inefficient nonlinear interaction with the excitation light (low two-photon absorption cross-sections, σ^2 < 100 GM, 1GM = 10^{-50}cm^{4}s),[14, 30, 31] and/or low emission quantum yields.[9, 32] The TPA-polymer has a maximum TPA cross-section of 6930 GM at 740 nm and emission centred at 520 nm, with a fluorescence quantum yield of 0.7.[22] In this paper, it is shown that the photoisomerization of PC can be induced indirectly upon excitation of the TPA-polymer via Förster resonance energy transfer (FRET). Volumetric data recording is demonstrated in a prototypical composite media.

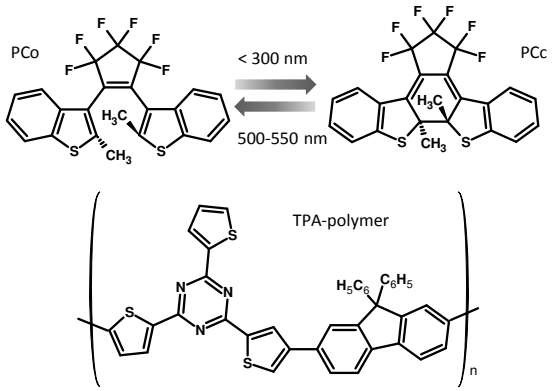

Fig. 1 Molecular structure of the two isomers of the photochromic and the TPA-polymer used in the storage media.

Experimental Section

Materials

The 1,2-bis(2-methylbenzo-[b]thiophen-3-yl)hexafluorocyclo-pentene (PC) unit and the linear polymer (TPA) with 2,4,6-tris(thiophen-2-yl)-1,3,5-triazine units bridged by 9,9-dihexyl-9H-fluorene have been synthesized as described earlier.[33,34] Data storage films where prepared from mixtures of the PC and TPA-polymer in an inert host matrix of ethyl cellulose (Sigma-Aldrich). Spectroscopic grade THF (Sigma-Aldrich) and Toluene (Sigma-Aldrich) were used as solvents.

Methods and Instrumentation

Steady state spectroscopy

The linear absorption spectra were recorded with a JASCO V-660 spectrophotometer. The fluorescence spectra were measured with a Horiba Jobin Yvon Fluorolog 3-22 Spectrofluorimeter with a Xenon lamp of 450 W.

Förster Resonance Energy Transfer efficiency

The Förster Resonance Energy Transfer efficiency (E_{FRET}=1-τ_{DA}/τ_D) was estimated from the average fluorescence decay times of the donor TPA-polymer measured in the presence (τ_{DA}) and absence (τ_D) of the closed form of the PC (PCc). Solutions with a constant concentration of the TPA-polymer (3×10^{-7} M) and a variable concentration of PCc (10^{-5}-10^{-3} M) were prepared in THF. The desired concentration of PCc was obtained from a solution of the ring opened form of the PC upon irradiation at 260 nm, under stirring and controlled temperature (22°C). The stationary state of PC was attained with approximately equal amounts of PC in the open and closed forms. The concentration of PCc in the stationary state was calculated by measuring its absorbance in a 1 cm path length quartz cuvette knowing the molar absorption coefficient at 525 nm (8.8 x 10^3 M^{-1}cm^{-1}).[30] The fluorescence decays were measured in 5 mm quartz cuvettes by the Single-Photon Timing technique under excitation of the TPA-polymer at 400 nm. The excitation source was the second harmonic of a tunable wavelength (700-1000 nm) Ti:Sapphire laser (Tsunami, Spectra Physics, Mountain View, CA) pumped by the second harmonic of a Nd:YVO4 laser (Milennia Xs, Spectra Physics, Mountain View, CA) delivering 100 fs pulses at a repetition rate of 80 MHz. A pulse-picker (Angewand Physik and Electronik) was used to reduce the repetition rate down to 4 MHz. The emission at 450 nm was collected at the magic angle by a Jobin Yvon HR320 monochromator (Horiba Jovin Ivon Inc.). The instrument response functions for deconvolution (35-80 ps FWHM) were generated by scattering dispersions of colloidal silica in water. The solutions were kept under gentle stirring during the data collection. Blank decays were acquired to ensure that dark photon counts were negligible. Decay curves were stored in 1024 channels with 6.11 ps/ channel and an accumulation of 20 kcounts in the peak channel. The fluorescence decays were analysed by a non-linear least-squares reconvolution method using the TRFA DP software by SSTC (Scientific Software Technologies Center, Belarusian State University, Minsk, Belarus).

Data recording and readout

The composite films for data storage were prepared using solutions of 2.5 wt% of ethyl cellulose (EC) in toluene with 0.1 wt% of the TPA-polymer and 1-12 wt% of PCc relative to ethyl cellulose. The solutions were stirred overnight and filtered through a membrane filter of PTFE with 0.2 µm pore size. These solutions were irradiated with the 450W Xenon lamp of the spectrofluorimeter at 260 nm, under stirring, until the photostationary state was reached. The solutions were then drop casted on glass cover slips and left to rest in an oven at 50°C until complete drying. For multilayer data storage, thicker films were prepared by casting several drops on the same spot of the cover slips. The films were stored in the dark to avoid external exposure to light.

The data recording and readout tests were made in a Leica TCS SP5 (Leica Mycrosystems CMS GmbH, Mannheim, Germany) inverted microscope (DMI6000) equipped with a CW Ar ion laser (458, 465, 488, 496 and 514 nm) and a tunable pulsed Ti:Sapphire laser (Spectra-Physics Mai Tai BB, 710-990 nm, 100 fs, 82 MHz). Typically, a HC PL FLUOTAR 50x 0.80 N.A. DRY objective was used, which results in diffraction limited excitation areas of FWHM of 0.61λ_{exc}/N.A. For two-photon

writing the excitation wavelength was 740 nm with excitation powers ranging from 0.4-6 MW/cm^2 (1-14 mW). The effect of exposure time on the bit profile was analysed by varying the exposure time from 1 to 1000 ms. The written bits were accessed by collecting fluorescence images in the 470-570 nm range under one-photon excitation at 458 nm with 1 KW/cm^2, or two-photon excitation at 740 nm (the same wavelength used in the writing process) with excitation fluences of ≈2 MW/cm^2. Images were collected with 1024×1024 pixels at typical scan rates of 400 Hz per frame, which corresponds to a pixel dwelling time of 2.4 µs. Under these conditions the emission is mainly due to the TPA-polymer. Due to the lack of a more suitable reading method, some degree of undesired writing during reading cannot be avoided, especially when one-photon excitation is used.

Photodecomposition

The photodecomposition quantum yield of the TPA-polymer was measured under one-photon excitation by UV-Vis absorption as described earlier.[35] The absorbance of a 0.14 µM solution of the TPA-polymer in THF, kept in a 5 mm path length quartz cuvette, was followed during irradiation at 400 nm, under stirring and constant temperature (22°C). The excitation source was the lamp of the spectrofluorimeter (450 W Xenon lamp with an intensity at 400 nm of 17 mW/cm^2). The excitation power was measured with a Si photodiode (Thorlabs, S121C and PM100D). The kinetics of photodecomposition in solution was followed by measuring the absorbance of the TPA-polymer at its absorption maximum (423 nm). The photodecomposition kinetics in optically thin films (0.1% in EC with optical density ≈ 0.1) was followed by fluorescence spectroscopy.[35] For one-photon decomposition, the excitation source is the lamp of the spectrofluorimeter. During irradiation the slits of the spectrofluorimeter are fully opened ensuring that all the volume of the sample is irradiated. Assuming that the photodecomposition products are not emissive at the same wavelength of the TPA-polymer, the photodecomposition kinetics in thin film was followed by collecting the fluorescence in front face geometry. The sample is kept in the same position inside the spectrofluorimeter during the measurements avoiding issues connected with reproducibility of sample positioning and inhomogeneity of solid samples. Due to the highly focused laser beam and reduced size of the excitation spot in two-photon excitation, the two-photon photodecomposition is even more influenced by such issues. Thus, the two-photon photodecomposition kinetics in thin EC films, was followed by counting the photons emitted from a diffraction limited spot generated by a 0.8 NA objective lens under excitation with 1 mW of pulsed light at 740 nm (similar condition to those used in writing operation). The epi-illumination microscope described above was used for excitation and collection of the emission. The number of photon per 100 ms was measured by an external PMT using a single-photon timing routine (Becker and Hickl, PMC-100-4 and SPC-830 acquisition board). The excitation source was the Ti-Sapphire laser used in the data recording and readout.

Results and discussion

Solid state optical properties

The absorption spectra of the open- (PCo) and closed-ring (PCc) forms of the PC in EC films are shown in **Fig. 2**. In agreement with the spectral features reported in solution, PCo absorbs in the UV range with maximum absorption wavelength at 260 nm, while PCc has an absorption band in the visible, centred at 525 nm.[28] Since the photochromic conversion requires minimal geometrical rearrangement as compared to other known photochromic process (e. g. cis-trans isomerization in azobenzene), this PC molecule shows photochromism even in the crystaline phase. Upon irradiation with UV light (≤ 300 nm), colorless solutions/films of the PCo become red due to the presence of PCc. The PC unit has no appreciable thermochromicity at moderatly high temperatures; the PCc form is stable for more than 3 months at 80°C, and the cyclization/ring-opening cycle can be repeated more than 10^4 times.[28, 29, 36]

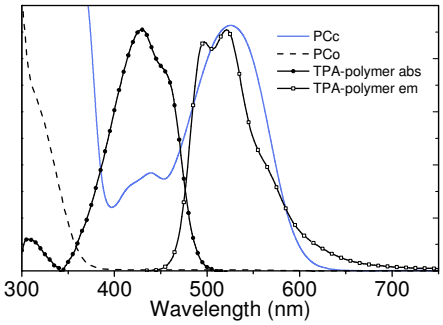

Fig. 2 Absorption spectra of the open- (PCo, dashed line)) and closed-ring (PCc blue line) forms of the PC and absorption (full circles) and emission (open squares) of the TPa-polymer in EC films.

The lowest energy absorption band of the TPA polymer in EC peaks at 423 nm (**Fig.2**), with the corresponding emission centred at 521 nm. The large spectral overlap between emission of the TPA-polymer and absorption of the PCc is shown in **Fig. 2**. While the reported TPA cross-section of the PC is rather low (85 GM at 520 nm for PCo and 120-150 GM for PCc in the 680-800 nm range)[14], the TPA cross-section of the TPA-polymer at 740 nm is 6930 GM.[22] Thus, excitation of the TPA at 740 nm in the presence of the PCc should result in energy transfer by FRET to the PCc, inducing the cycloreversion process. An efficient FRET process is expected to quench the emission of the TPA-polymer in the presence of PCc (an illustration of the FRET induced writing is presented in the ESI). Once PCc is converted into PCo, the emission of the TPA-polymer is recovered.

FRET efficiency

In the following section the FRET efficiency between the TPA unit (donor, D) and the PCc (acceptor, A) is evaluated and rationalized in the context of the Förster theory. The rate of energy transfer from a donor to an acceptor is $k_T(r) = \frac{1}{\tau_0}(R_0/r)^6$, in which r is the separation between donor and acceptor molecules and R_0 is the Förster radius. R_0 can be determined from spectroscopic data as follows [37]:

$$R_0^6 = \frac{9ln(10)\kappa^2\Phi_D^0}{128\pi^5 N_A n^4} J \quad (1)$$

where κ^2 is the transition dipole moments orientation factor ($\kappa^2 = 2/3$ in the fast rotational diffusion limit), Φ_D^0 is the fluorescence quantum yield of the donor in the absence of energy transfer, n is the refractive index of the medium, N_A is the Avogadro number and J is the spectral overlap integral given by:

$$J = \int F_D(\lambda)\varepsilon_A(\lambda)\,\lambda^4 d\lambda \quad (2)$$

$F_D(\lambda)$ is the normalized emission spectrum of the excited donor and $\varepsilon_A(\lambda)$ is the molar absorption coefficient of the acceptor ($M^{-1}cm^{-1}$). The one-photon fluorescence quantum yield of the TPA-polymer and the calculated overlap integral used to estimate R_0 in solution and in film are given in Table 1.

Table 1. Fluorescence quantum yield of the TPA polymer (Φ_D^0) and overlap integrals (J) used in the calculation of the Förster radius (R_0) for the TPA-polymer/PCc donor/acceptor pair in solution and in the data storage film with 1% PCc.

	solution (THF)	film
Φ_D^0	0.71[a]	0.59[b]
τ_F (ns)	0.89	0.51
$J\times10^{15}$ ($M^{-1}cm^3$)	42.3	47.1
R_0 (Å)	40.6	38.9

[a]Measured with excitation at 370 nm using quinine as a standard (Φ=0.57). [b]Measured with excitation at 460 nm using Rhodamine 6G (Φ=0.94) as reference.

Both the calculated Förster radius in solution and in film are ≈ 40 Å. The lower fluorescence quantum yield of the TPA-polymer in the data storage films is compensated by the stronger overlap integral due to a red-shift of the emission spectrum in the film, with respect to the solution. R_0 values of the same order have been previously reported in donor-acceptor pairs comprised of different fluorene derivatives as TPA donors combined with different photochromic diarylethene as acceptor.[14, 17]

The value of R_0 and the critical acceptor concentration (A_0), can also be determined experimentally by evaluation of the dependence of the FRET efficiency on the acceptor concentration. The transfer efficiency, E, was calculated by using the average decay times of the donor in the absence ($\bar{\tau}_D$) and presence of the acceptor ($\bar{\tau}_{DA}$) as follows:[37]

$$E = 1 - \frac{\bar{\tau}_{DA}}{\bar{\tau}_D} \quad (3)$$

The fluorescence decay of the TPA polymer is multiexponential, with different decay components resulting from the complexity of the excited state processes in polymeric systems. Four exponentials are needed to fully describe the fluorescence decays. In spite of the complex lifetime, time-domain measurements, as opposed to integrated emission measurements (quantum yields) , are here discussed because they are much less prone to artefacts such as light scattering, inner-filter effects, bleaching or contamination with autofluorescence.

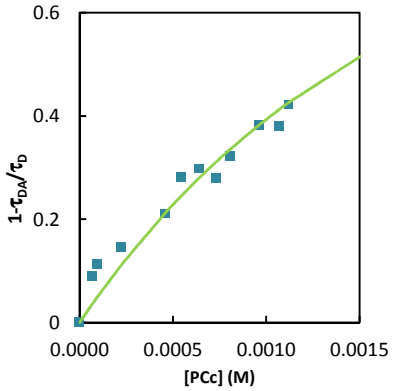

Fig. 3 Dependence of the FRET efficiency on the concentration of PCc (acceptor molecule) in THF solution. Symbols are experimental points and the straight line is the fitted curve according to eq. 4. The fitted curve corresponds to A_0 of 3.2×10^{-3} and R_0=52 Å. A significant deviation of the fitted curve from the experimental points was observed at higher concentration of acceptor (not shown) due to aggregation effects.

The energy transfer efficiency was fitted by equation (4):

$$E = 1 - \frac{\bar{\tau}_{DA}}{\bar{\tau}_D} = \sqrt{\pi}.\gamma.exp(\gamma^2).[1 - \mathrm{erf}(\gamma)] \quad (4)$$

with $\gamma = A/A_0$, where A is the acceptor concentration and the critical concentration A_0 (in M) relates to the Förster radius[37, 38] by

$$A_0 = 447/R_0^3 \quad (5)$$

$$erf(\gamma) = \frac{2}{\sqrt{\pi}}\int_0^{\gamma} exp(-x^2)dx \quad (6)$$

Equation 4 is valid for static and homogeneously distributed donors and acceptors. As shown in **Fig. 3**, a reasonably good fit of the experimental data is obtained using eq. 4 with a R_0= 52 Å. The difference in the calculated (Table 1) and experimental values of R_0 might be associated with the multiexponential lifetime of the donor in the absence of acceptors and the possibility of molecular diffusion during the donor lifetime, not considered in the Förster's model as expressed by Eq. 4. Based on the experimental R_0 value, a critical acceptor concentration of A_0 =3.2×10^{-3} M is estimated. This concentration is similar to the value reported earlier for donor-acceptor pairs comprised of different fluorene derivatives as TPA donors combined with the same PC compound as acceptor (6.8×10^{-3} M).[14] To guarantee a high FRET efficiency, the concentration of PCc in the data storage medium was chosen so as to correspond to a distance between acceptors that does not exceed the estimated Förster radius. The kinetics of cycloreversion, with and without TPA-polymer, shows that the FRET induced cycloreversion by two-photon excitation at 740 nm in the presence of the TPA-polymer enhances the photoconversion rate (Fig. S2 in the ESI).

Optical memory operation

The unexposed data storage film is composed of a mixture of PCc and PCo, with approximately equal concentrations, and

TPA-polymer embedded in an inert polymer matrix. The weight percentage of the TPA-polymer relative to the inert polymer was fixed at 0.1%. The typically used weight percentages of PCc in unexposed films where 1-12%, which resulted in an average separation between PCc molecules of 52-22 Å. As a result of the efficient quenching of emission of the TPA-polymer by the PCc, the unexposed film is a dark matrix, that becomes fluorescent only at the irradiation volume, where the two-photon FRET-assisted cycloreversion is induced upon excitation at 740 nm. Reading can be done by collecting the emission of the TPA-polymer in the 470-570 nm range, either upon one- (λ_{exc}= 458 nm) or two-photon excitation (λ_{exc}= 740 nm). In the read process, a considerably lower power and/or lower exposure times are used when compared to the write process.

The nonlinearity of the writing process was checked by irradiating a given area of the data storage film at 740 nm with laser powers ranging from 2.5 to 20 mW, during a fixed time (**Fig. 4**). The linearity of the log-log plot of the integrated up-converted fluorescence intensity as a function of the excitation power, and the slope of ≈2, confirm the nonlinearity of the writing process (**Fig. 4**).

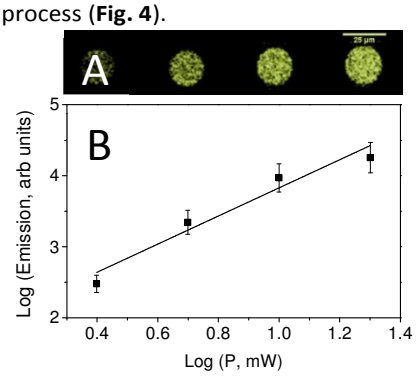

Fig. 4 Fluorescence image (A) and graphic representation (B) of the integrated fluorescence intensity of the TPA-polymer in the storage film (0.1% TPA and 4% PCc) as a function of laser intensity at 740 nm. The emission intensity upon excitation at 458 nm was collected using a 0.8 NA dry objective.

The properties of the written bit (FWHM and intensity in xy-plane perpendicular to the optical axis) have been studied as a function of the exposure time (1-1000 ms) under 1 mW excitation at 740 nm (0.4MW/cm^2 for the 0.8 NA objective). **Fig. 5** shows the bit properties as addressed by two-photon excitation at the same wavelength, with the same objective, using higher excitation powers (4.5 mW) and pixel dwelling time in the microsecond range. Both FWHM and intensity increase exponentially with the exposure time. Using such readout conditions, the signal to noise ratio is 2 at 1ms, it improves to 4.6 at 50 ms and, due to signal saturation, it reaches a limiting values of 12 for 1000 ms of exposure time. A contrast similar to the one achieved in composite films reported earlier operating on the same principle has been achieved here with five times lower excitation fluence and three orders of magnitude lower exposure times, as compared.[14] We checked that, for data storage films composed only of the PC,[9] exposure times three orders of magnitude longer and one order of magnitude higher powers are required to get bits with a similar signal-to-noise ratio.

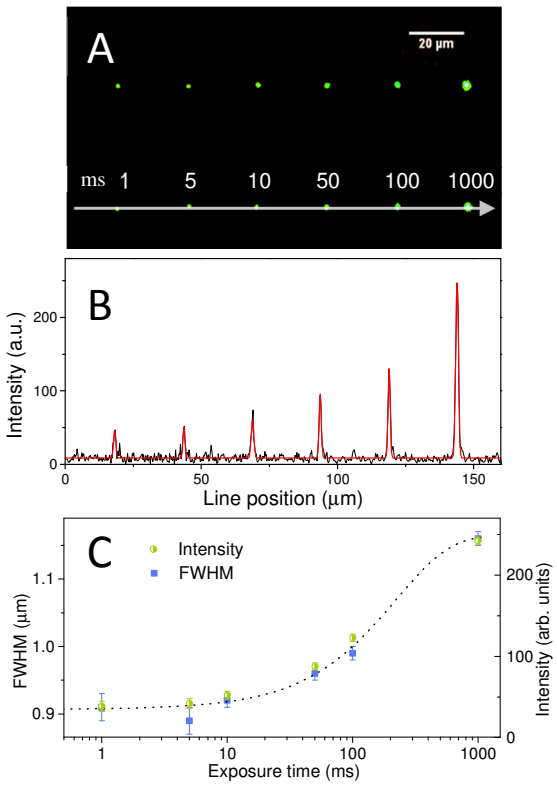

Fig. 5 Bit profile in the xy-plane, perpendicular to the optical axis, as a function of the exposure time. (A) Microscope image of data bits recorded by two-photon excitation at 740 nm and 1 mW at different exposure times. The readout was done by two-photon excitation at 740 nm and 4.5 mW using a 0.8 NA objective lens, with pixel dwelling times of 2.4 µs (250x250 mm, 1024x1024 pixels and 400Hz of line rate). Panel (B) shows the intensity profile along the arrow in panel (A) and the corresponding fit to Gaussian functions. The peak intensity and the FWHM of each function is shown in panel (C). The dotted line is an eye guiding line that evidences the exponential nature of the dependence of the intensity and FWHM with the exposure time.

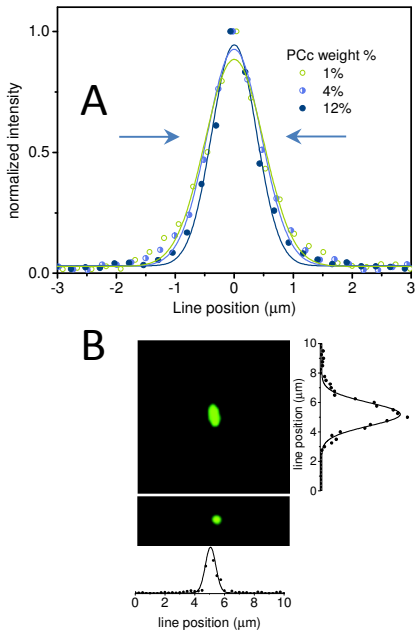

Fig. 6 Intensity profile of the bit as a function of PCc weight percentage. The radial intensity profile (profile along a line drawn in the xy-plane crossing the center of the bit) is shown in panel (A). Panel (B) shows and 10x10 µm image of the smallest bit together with its radial (xy) and axial (xz) intensity profile.

In **Fig 5**, it is puzzling that the FWHM of the written bits seems to converge to a minimum value of 0.91 µm, well above the diffraction limit. The FWHM of the Point-Spread-Function (PSF), as routinely measured by imaging fluorescent beads of subresolution dimension (100 nm), is 0.47 µm and 0.89 µm in the xy- and xz-planes, respectively. Thus, the narrowest bits have nearly twice the FWHM of the PSF of the system. The width of the bit cannot be limited by exciton diffusion by FRET due to the small R_0 values (with R_0 of 4-5 nm the FRET efficiency drops to ≈ 2% at a distance of 10 nm from the primary singlet exciton generated on the TPA-polymer). This argument excludes also homo-transfer among individual TPA-polymer chains and among individual PC molecules. Exciton diffusion on the micrometer range can only be understood in terms of radiative energy transfer (RET) from the TPA-polymer to the PCc molecules. FRET and radiative energy transfer (RET) occur simultaneously and depend on similar parameters such as the spectral overlap integral between donor emission and acceptor absorption and the concentration of acceptor. The contribution of each process for the efficiency of energy transfer depends on the acceptor concentration, RET dominates for low acceptor concentrations, while for high acceptor concentrations it can be negligible. RET is governed by the Beer-Lambert law and so it strongly depends on the optical path. The attenuation length, which is the distance at which the intensity of the excitation beam has dropped by to 1/e, is inversely proportional to the concentration. This means that, in the event of exciton diffusion by RET, the bit width should decrease with an increase on the concentration of PCc. **Fig. 6** shows that increasing the concentration of PCc from 1-12% reduced the bit width from 1.1-0.9 µm. The smallest bit that can be read in our system was written in a 12% PCc film upon excitation at 740 nm, with the shortest exposure time (1ms) and an excitation power of 1mW with a 0.8 NA dry objective lens (**Fig. 6**). This bit has ≈0.9 and 1.3 µm of FWHM in the xy- and xz-plane, respectively (**Fig. 6**). It is noteworthy that in the 12 % PCc film, with an average distance between acceptors of roughly half of the R_0 value, the expected FRET efficiency based on a homogeneous distribution of the donor and acceptors should be nearly 100%. Thus, almost no light should be emitted by the TPA-polymer that could be re-absorbed by the PCc, and the bit width should approach the width of the PSF. Since that is not the case, the FRET efficiency in the film must be lower than expected in order for the radiative transfer to be a competitive process. The FRET efficiency should be of the same order of the probability of absorption by PCc of the radially emitted radiation by the TPA-polymer, which is ≈30% over a distance of 1 µm in a 12% PCc film. The reduced FRET efficiency can be due to inhomogeneity of the composite film, which can result from aggregation of the the PCc. One way to overcome such adverse effects can be the covalent linkage of PCc units to the TPA-polymer.

As a proof of concept, the two-photon 3D-recording and readout ability of the composite film is illustrated in **Fig. 7.** Three layers of bits where recorded in a 60 µm thick film, separated by 15 µm with a distance of 50 µm between neighbouring bits in each layer. The exposure time for writing was 10 ms and the excitation power 13 mW. Up to four layers were obtained in some samples, the number of layers being limited by the thickness of the film obtained with the drop-cast method.

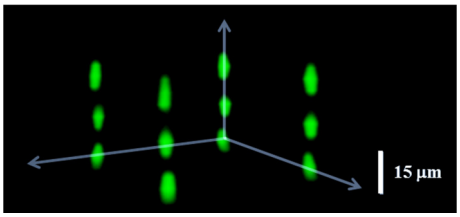

Fig. 7 3D image of three layers of bits recorded by two-photon excitation at 740 nm (13 mW, 10 ms of exposure time) and readout at the same excitation wavelength using a lower power (5 mW, 400HZ 155 x 155 x 1000 nm voxel size). The 3D image is reconstructed from 50 consecutive layers separated by 1 µm. The consecutive layers are separated by 15 µm and the neighboring bits on each layer are 50 mm far apart

Photobleaching of TPA-polymer

In this section the photostability of the TPA-polymer, under one-photon (400-423 nm) and two-photon (740 nm) excitation in solution and in thin film, is discussed. The PC unit has been proven to be photostable, allowing for more than 14000 cycles of cyclization/cycloreversion without appreciable photo-bleaching.[28] Thus, it is the stability of the TPA-polymer that will determine the resistance to fatigue of the system. The one-photon photodecomposition quantum yields were determined using both the absorption (in solution) and the fluorescence methods (in film) as described earlier.[35]

The decay of the absorption of the TPA-polymer in diluted THF solutions upon excitation at 423 nm is shown in Fig. S3 of the ESI. The one-photon photodecomposition quantum yield extracted from these data was ≈ $4x10^{-8}$. This result compares favourably with the values of the order of 10^{-5} reported earlier for different fluorene derivatives in solution.[39] It compares also favourably with the $4x10^{-6}$ quantum efficiency of photodecomposition of Rhodamine 6G in methanol. Rhodamine 6G is a dye used in commercial lasers due to its photostability and high emission quantum yields, that is here used to validate the method. The values reported earlier for this dye in diluted solutions are also in the 10^{-6} range.[40]

The absorption method is not suitable to follow the photodecomposition kinetics in solid samples due to the lack of reproducibility of sample positioning when shuttling between the absorption measurement in the UV-vis absorption spectrophotometer and excitation in the spectrofluorimeter. Alternatively, the photobleaching in EC films was determined by the fluorescence method, whereby the photodecomposition is followed by collecting the emission of an optically thin film (0.1% of TPA-polymer in EC with optical density ≈0.1) in a front face geometry. The sample remains in the spectrofluorimeter during collection of the kinetic data. The decay of the fluorescence of the TPA-polymer in the film, upon excitation at 400 nm, is shown in Fig. S3 of the ESI. The one-photon photodecomposition quantum yield extracted from these data was $3x10^{-6}$, considerably higher than in solution, but still quite low.

Guaranteeing the stability of sample positioning with respect to the laser beam is even more important in the determination of the two-photon photodecomposition quantum yields in the solid state, due to the reduced size of the laser beam and inhomogeneity in the film. This is particularly difficult when the excitation area is reduced to the diffraction limited excitation spot generated by the typically high numerical aperture lenses used in the operation of optical memories (excitation areas of the order of/or less than 1 μm^2). Thus, the kinetics of the fluorescence decay in the solid state under two-photon excitation was followed by measuring the rate of photons emitted in front face geometry by the TPA-polymer under excitation at 740 nm within the diffraction limited spot generated by a 0.8 NA objective lens. The evolution of the count rate is shown in **Fig. 8** for the TPA-polymer in comparison with Rhodamine 6G. The photostability of the TPA-polymer is about two-orders of magnitude higher than that of the Rhodamine 6G dye. In the TPA-polymer, the photon count decreases by 50% after 22s of irradiation but it remains higher ($6.6x10^{-4}$ counts/s) than that of Rhodamine 6G ($1.5x10^{-4}$ counts/s). If 1ms is used in the writing process, 22000 writing operations could be performed during such time. We estimate that about the same number of reading operations would be necessary to reduce the bit depth by 50%. In a conservative estimate, assuming the kinetics of photodecomposition of the TPA-polymer during the erasing process to be similar to the writing process, 5000 write-read-erase cycles would lead to a reduction of the bit depth by 50%.

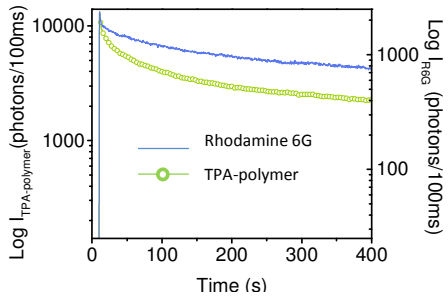

Fig. 8 Two-photon bleaching kinetics of the TPA-polymer and Rhodamine 6G in films (0.1% in EC, λ_{exc}= 740 nm, I_0≈0.4 MW/cm^2 corresponding to 1 mW in the diffraction limited spot of the 0.8 NA objective lens).

Conclusions

The 2,4,6-tris(thiophen-2-yl)-1,3,5-triazine core was demonstrated to be an efficient framework in the design of nonlinear functional materials. Multilayer data storage was demonstrated in composite films of photochromic molecules doped with a polymer composed of alternating 2,4,6-tris(thiophen-2-yl)-1,3,5-triazine units bridged by 9,9-dihexyl-9H-fluorene. Due to its high two-photon absorption, the polymer acts as a nonlinear NIR-antenna. Volumetric data recording with as little as 1 ms of exposure time and 1mW of 740 nm radiation was accomplished. In such conditions, the two-photon excitation of the polymer triggers a unidirectional isomerization of the PC molecules (a cycloreversion process from the closed to the open isomer) via FRET. An exposure time three orders of magnitude longer and one order of magnitude higher powers are required to get similar signal-to-noise ratio in a data storage film composed only of the PC. In the storage media, the observed FRET efficiency was lower than expected due to inhomogeneity of the composite film. Increasing the FRET efficiency would lead to shorter exposure times for both writing and reading operations, thus increasing the number of memory cycles. The best strategy to achieve this goal would be to reduce the distance between donor and acceptors by covalently linking the PC unit to the TPA-polymer.

Acknowledgements

We acknowledge financial support from Fundação para a Ciência e a Tecnologia (Post-doc grant SFRH/BPD/75782/2011, SFRH/BPD/88666/2012, PhD grant SFRH/BD/67025/2009, SFRH/BPD/100677/2014 and IF/00759/2013, projects PTDC/CTM-POL/114367/2009, RECI/CTM-POL/0342/2012).

References

1 P. Hanczyc, M. Samoc and B. Norden, *Nat. Photonics*, 2013, **7**, 969-972.
2 S. Yao and K. D. Belfield, *Eur. J. Org. Chem.*, 2012, 3199-3217.
3 P. Bianchini, B. Harke, S. Galiani, G. Vicidomini and A. Diaspro, *P. Natl. Acad. Sci. USA*, 2012, **109**, 6390-6393.
4 K. Konig, *J. Microsc.*, 2000, **200**, 83-104.
5 P. A. Bouit, G. Wetzel, G. Berginc, B. Loiseaux, L. Toupet, P. Feneyrou, Y. Bretonniere, K. Kamada, O. Maury and C. Andraud, *Chem. Mater.*, 2007, **19**, 5325-5335.
6 S. Kawata and Y. Kawata, *Chem. Rev.*, 2000, **100**, 1777-1788.
7 A. B. Taylor and J. W. M. Chon, *Adv. Opt. Mat.*, 2015, **3**, 695-703.
8 F. Q. Guo, J. Hu, B. Guo and H. Liang, in *New Materials and Processes, Pts 1-3*, eds. W. Z. Chen, Q. Li, Y. L. Chen, P. Q. Dai and Z. Y. Jiang, 2012, vol. 476-478, pp. 1245-1248.
9 E. Samoylova, W. Dallari, M. Allione, F. Pignatelli, L. Marini, R. Cingolani, A. Diaspro and A. Athanassiou, *Mat. Sci. Eng. B-Adv.*, 2013, **178**, 730-735.
10 J. Lott, C. Ryan, B. Valle, J. R. Johnson, D. A. Schiraldi, J. Shan, K. D. Singer and C. Weder, *Adv. Mater.*, 2011, **23**, 2425-2429.
11 P. Zijlstra, J. W. M. Chon and M. Gu, *Nature*, 2009, **459**, 410-413.
12 E. Walker, A. Dvornikov, K. Coblentz and P. Rentzepis, *Appl. Opt.*, 2008, **47**, 4133-4139.
13 A. S. Dvornikov, E. P. Walker and P. M. Rentzepis, *J. Phys. Chem. A*, 2009, **118**, 13633-13644.
14 C. C. Corredor, Z.-L. Huang, K. D. Belfield, A. R. Morales and M. V. Bondar, *Chem. Mater.*, 2007, **19**, 5165-5173.
15 G. Fuxi and W. Yang, eds., *Data Storage at the Nanoscale: Advances and Applications*, Taylor & Francis Group LLC, 2015.
16 G. Bort, T. Gallavardin, D. Ogden and P. I. Dalko, *Angew. Chem. Int. Edit.*, 2013, **52**, 4526-4537.

17 K. D. Belfield, M. V. Bondar, C. C. Corredor, F. E. Hernandez, O. V. Przhonska and S. Yao, *ChemPhysChem*, 2006, **7**, 2514-2519.
18 T. J. Mooibroek and P. Gamez, *Inorg. Chim. Acta*, 2007, **360**, 381-404.
19 P. Gamez and J. Reedijk, *Eur. J. Inorg. Chem.*, 2006, 29-42.
20 D. F. Sun, S. Q. Ma, Y. X. Ke, T. M. Petersen and H. C. Zhou, *Chem Commun*, 2005, 2663-2665.
21 P. Zhou, C. Zhong, X. Chen, J. Qin, I. F. A. Mariz and E. Macoas, *Macromol.*, 2014, **47** 6679–6686.
22 I. F. A. Mariz, E. M. S. Maçoas, J. M. G. Martinho, L. Zou, P. C. Zhou, X. G. Chen and J. G. Qin, *J. Mat. Chem. B*, 2013, **1**, 2169-2177.
23 L. Q. Zhang, L. Zou, J. Xiao, P. C. Zhou, C. Zhong, X. G. Chen, J. G. Qin, I. F. A. Mariz and E. Macoas, *J. Mat. Chem.*, 2012, **22**, 16781-16790.
24 L. Zou, Y. Liu, N. Ma, E. Macoas, J. M. G. Martinho, M. Pettersson, X. G. Chen and J. U. Qin, *Phys. Chem. Chem. Phys.*, 2011, **13**, 8838-8846.
25 Y.-Z. Cui, Q. Fang, Z.-L. Huang, G. Xue, G.-B. Xu and W.-T. Yu, *J. Chem. Mat.*, 2004, **14**, 2443-2449.
26 Z. J. Liu, T. Chen, B. Liu, Z. L. Huang, T. Huang, S. Y. Li, Y. X. Xu and J. G. Qin, *J. Mat. Chem.*, 2007, **17**, 4685-4689.
27 F. Xu, Z. Wang and Q. Gong, *Opt. Matt.*, 2007, **29**, 723-727.
28 M. Hanazawa, R. Sumiya, Y. Horikawa and M. Irie, *J. Chem. Soc.Chem. Comm.*, 1992, 206-207.
29 M. Irie, *Chem. Rev.* , 2000, **100**, 1685–1716.
30 C. C. Corredor, K. D. Belfield, M. V. Bondar, O. V. Przhonska and S. Yao, *J. Photoch. Photobiol. A*, 2006, **184**, 105-112.
31 Y. Feng, Y. Yan, S. Wang, W. Zhu, S. Qian and H. Tian, *J Mat. Chem.*, 2006, **16**, 3685-3692.
32 G. Luchita, M. V. Bondar, S. Yao, I. A. Mikhailov, C. O. Yanez, O. V. Przhonska, A. E. Masunov and K. D. Belfield, *Acs Appl. Mat. Interf.*, 2011, **3**, 3559-3567.
33 M. Irie, O. Miyasake, K. Uchida and T. Eriguchi, *J. Am. Chem. Soc.*, 1994, **116**, 9894-9900.
34 L. Zou, Y. Fu, X. Yan, X. Chen and J. Qin, *J. Polym. Sci.*, 2008, **46**, 702-712.
35 K. D. Belfield, M. V. Bondar, Y. Liu and O. V. Przhonska, *J. Phys. Org. Chem.*, 2003, **16**, 69-78.
36 M. Irie, *Pure and Appl. Chem.*, 1996, **68**, 1367-1371.
37 B. Valeur and M. N. Berberan-Santos, *Molecular Fluorescence*, Wiley-VCH Verlag GmbH, Weinheim (Germany), 2nd ed. edn., 2012.
38 R. Lakowicz, *Principles of Fluorescnece Spectroscopy*, Springer, Baltimore, USA, 3rd edn., 2006.
39 K. D. Belfield, M. V. Bondar, O. V. Przhonska and K. J. Schafer, *J. Photochem. Photobiol. A*, 2004, **162**, 489-496.
40 C. Eggeling, A. Volkmer and C. A. M. Seidel, *ChemPhysChem*, 2005, **8**, 791-804.

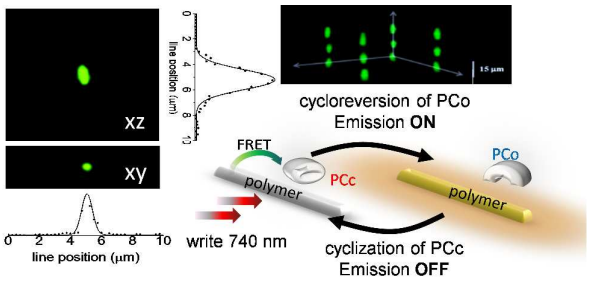

Multilayer data storage is demonstrated in films of photochromic (PC) molecules doped with a nonlinear NIR-antenna polymer based on triazine